

Determination of the absolute rate constant for associative ionization in crossed-beam collisions between Na $3^2P_{3/2}$ atoms

Regina Bonanno, Jacques Boulmer,* and John Weiner

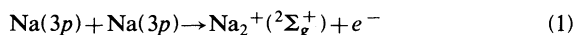
Department of Chemistry, University of Maryland, College Park, Maryland 20742

(Received 31 January 1983)

We report the determination of the absolute rate constant of Na_2^+ production by associative ionization collisions between crossed beams of Na $3^2P_{3/2}$ atoms. New measurement techniques greatly improve the accuracy of rate-constant determinations in crossed-beam experiments. We find the rate constant to be $(1.8 \pm 0.7) \times 10^{-11} \text{ cm}^3 \text{ sec}^{-1}$. This value is appreciably larger than many of those previously reported.

I. INTRODUCTION

The production of Na_2^+ in associative ionization (AI) collisions between two Na $3p$ atoms



has been the subject of considerable study in recent years.¹⁻⁴ Much of the interest in this and similar alkali-metal vapor ionization processes has centered on their role in the production of seed electrons. These electrons become collisionally superheated and initiate cascade processes leading to highly ionized alkali-metal vapors.⁵

Previously reported cross sections for (1) have varied over several orders of magnitude from 10^{-15} – 10^{-18} cm^2 .¹⁻⁴ Two principal sources of error can account for such a wide disparity. The first is in the extraction and detection of the Na_2^+ ions, which generally introduce certain apparatus constants that are often difficult to measure and subject to large uncertainties. The second source lies in the determination of the Na $3p$ number density. Common methods include ion impact and surface ionization,¹ fluorescence measurements,² and equilibrium vapor-pressure determinations in cell experiments.⁶ For these methods to give accurate results it is critical that the experimental conditions are well defined and measured. In this paper we present a new approach which greatly reduces these problems and provides a means to accurately determine the rate constant for the $3p$ - $3p$ AI process.

II. APPARATUS DESCRIPTION

Figure 1 is a schematic diagram of the experimental setup. Although the basic apparatus has recently been described in detail,⁷ a brief description will be given here for the sake of clarity. Two effusive atomic-beam sources, in the horizontal plane at 90° to each other, enter the vacuum chamber and intersect in a well-defined collision volume. The laser axis is in the same plane as the sources and bisects the angle between them. A tunable flash-lamp pumped dye laser (laser 1) excites the Na $2^2P_{3/2}$ level from which reaction (1) takes place. Determination of the Na $3p$ number density involves direct photoionization of the excited Na atoms. To produce the photoionizing uv pulse, we generate the second harmonic of the visible output from the Nd³⁺:YAG pumped dye laser (laser 2). Dia-

phragms spatially limit and define both laser beams before they enter the chamber.

As indicated in Fig. 1, ions produced synchronously with the laser pulse are accelerated vertically through a 15-cm time-of-flight (TOF) drift tube and detected by a particle multiplier. The acceleration field is pulsed on approximately 20 nsec after the arrival of the laser pulse and remains on for a 2 μsec duration. The amplitude of the electric field is no more than 24 V/cm. We place a pulsed suppressor grid immediately before the particle multiplier, which selectively blocks very large early arriving ion bunches. This allows us to measure higher mass but lower intensity peaks without electronic distortion. This feature is especially useful for measuring a weak Na_2^+ signal in the presence of a strong Na⁺ intensity. Signal output from the particle multiplier is buffered, amplified, and fed to a gated integrator.

Lasers 1 and 2 are synchronized and the delay between them can be continuously adjusted from 0–1500 nsec with a time jitter of less than 1 nsec. We select a 300-nsec segment of the relatively long pulse ($\sim 1 \mu\text{sec}$) from laser 1 by using a Pockels cell optical shutter. The duration of the pulse is adjustable from 10–300 nsec and the rising and falling edges are defined to within 2 nsec.

Also shown in Fig. 1 are a channel-electron multiplier (CEM) and photon collection optics which, although not used in these experiments, allow us to monitor electron and photon production in ionization processes.

III. EXPERIMENTS

The rate equation that governs the formation of Na_2^+ from AI is

$$\frac{d[\text{Na}_2^+]}{dt} = k [\text{Na}(3p)]^2, \quad (2)$$

where bracketed quantities represent number densities and k is the AI rate constant. Integration of Eq. (2) over the time of Na_2^+ production yields

$$k = \frac{[\text{Na}_2^+]}{[\text{Na}(3p)]^2 \Delta t}. \quad (3)$$

Therefore, we can readily calculate the rate constant with a knowledge of the Na_2^+ and Na $3p$ densities. In any experiment, the time-integrated Na_2^+ ion signal will be pro-

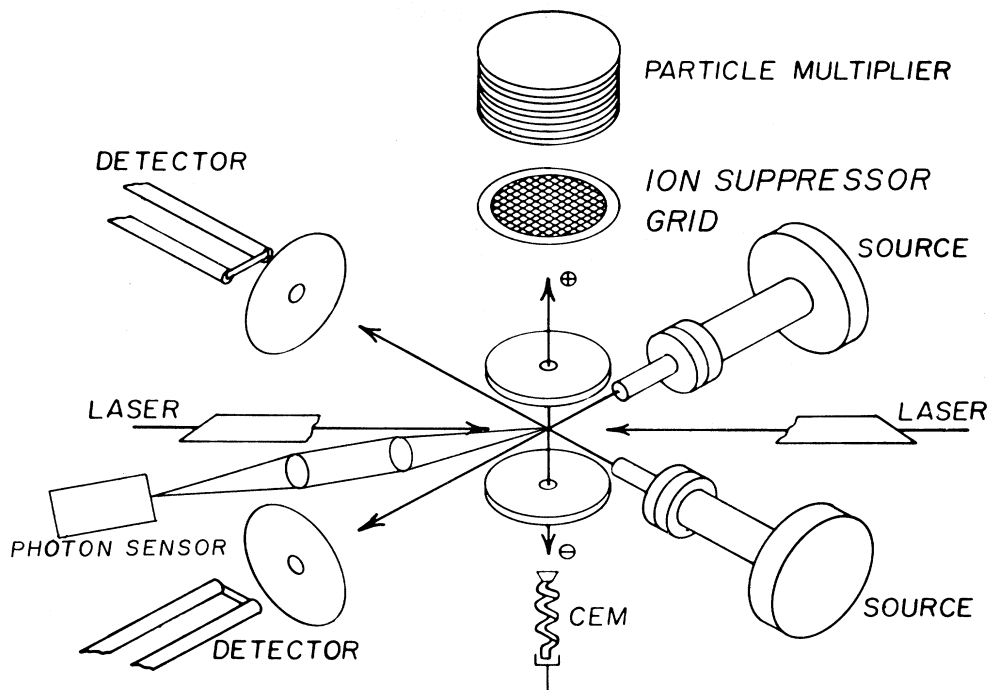
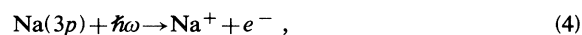


FIG. 1. Schematic diagram of the apparatus. Interaction region is completely surrounded by liquid-nitrogen-cooled baffles. Gated suppressor grid blocks distortion of weak Na_2^+ signals from strong Na^+ intensity.

portional to the Na_2^+ density, with the proportionality factor being those constants associated with the extraction and detection of the ions. These constants include ion collection efficiency, quantum efficiency and gain of the particle multiplier, and effective collection volume, as well as electronic factors associated with signal processing. The technique that we present here eliminates the necessity to know or determine all but one of these constants. After measuring the Na_2^+ AI signal, we measure an Na^+ ion signal due to direct photoionization out of the saturated $\text{Na } 3p$ level. This photoionization signal is acquired under identical conditions and during the same experimental run as the Na_2^+ AI signal. The ratio $[\text{Na}_2^+]/[\text{Na}^+]$ will then be independent of all constants relating to the ion detection and extraction with the exception of the effective collection volume. We verified that the ion collection efficiency was the same for Na^+ and Na_2^+ by performing two tests: First, the pulsed-ion-extraction field was varied in amplitude over a factor of 5, and it was observed that although the intensity increased somewhat, the ratio of Na^+ to Na_2^+ remained unchanged. Second, we directly photoionized Na and Na_2 in the effusive alkali-metal beam at fixed temperature. From the measured Na^+ and Na_2^+ intensities and known photoionization cross sections we calculated the fractional monomer and dimer populations. The results were in excellent agreement with monomer-dimer fractions calculated from thermodynamic data.

Owing to diffusion of imprisoned resonance radiation, the interaction volume for AI is always greater than the laser-beam cylinder and quite sensitive to Na density.⁸ Therefore the effective interaction volume for AI must be

measured directly in a separate experiment as described later. By contrast, the effective volume of Na^+ generated by photoionization of $\text{Na } 3p$ atoms is essentially determined by the geometric beam cylinder of laser 2. We take advantage of the fact that direct photoionization of the atoms in the $3p$ level,



generates a signal proportional to the $\text{Na } 3p$ density. The rate equation for the photoionization is

$$\frac{d[\text{Na}^+]}{dt} = \sigma_i[\text{Na}(3p)]I, \quad (5)$$

where I is the photon flux of the photoionizing laser (photons/cm²sec) and σ_i is the photoionization cross section (cm²). Integrating Eq. (5) over time, we find the $\text{Na } 3p$ density is given by

$$[\text{Na}(3p)] = \frac{[\text{Na}^+]}{\sigma_i\Phi} \quad (6)$$

where Φ is the radiation density in photons/cm². Combining Eqs. (3) and (6) we obtain

$$k = \frac{[\text{Na}_2^+]}{[\text{Na}^+]} \frac{\sigma_i\Phi}{[\text{Na}(3p)]\Delta t}. \quad (7)$$

Since the quantities $[\text{Na}_2^+]$ and $[\text{Na}^+]$ are both functions of the same apparatus constants, the ratio of the ion densities, $[\text{Na}_2^+]/[\text{Na}^+]$ can be reduced to the ratio of $I_{\text{Na}_2^+}/I_{\text{Na}^+}$, where $I_{\text{Na}_2^+}$ and I_{Na^+} represent the integrated ion signals per unit volume. Thus, the equation for the

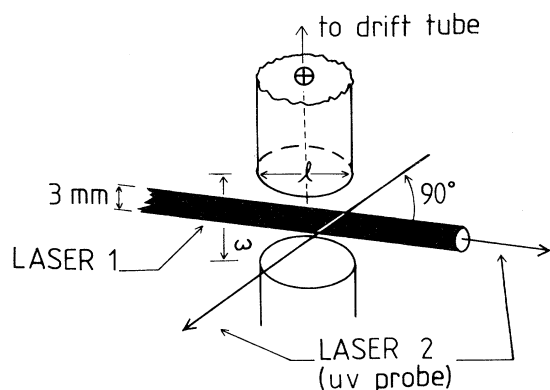


FIG. 2. Schematic illustrates the technique used to determine the effective volume of excited Na $3p$ atoms produced by laser 1. The uv probe (laser 2) is used to photoionize $3p$ atoms in the interaction region. By systematically varying the position of the probe in this region while monitoring the Na^+ intensity, we obtain a three-dimensional spatial distribution which is a direct measure of the excited-atom volume.

rate constant can be rewritten

$$k = \frac{I_{\text{Na}_2^+}}{I_{\text{Na}^+}} \frac{\sigma_i \Phi}{[\text{Na}(3p)] \Delta t} \quad (8)$$

We cannot directly replace the ratio of the ion number densities in Eq. (7) with the ratio of the time-integrated ion signals because the effective volume over which we collect the ions is different for Na_2^+ and Na^+ . The volume for Na^+ is defined by the effective volume swept

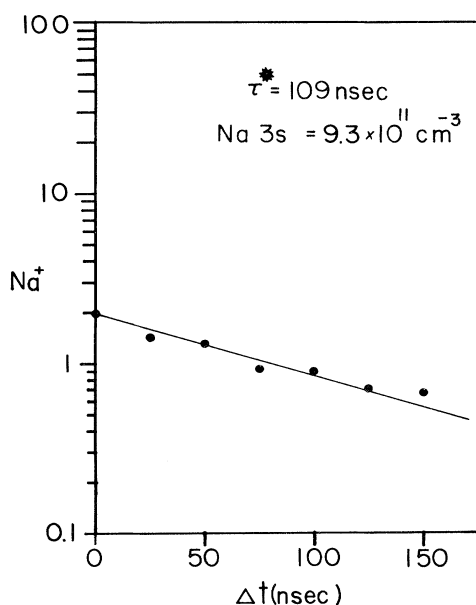


FIG. 3. Log-linear plot of the Na^+ signal (arb. units) vs time delay between lasers 1 and 2. Na^+ signal, generated by direct photoionization of atoms in the $3p$ level, is proportional to the $3p$ population. Slope is equal to $[1/(2.303)]\tau^*$.

out by the photoionizing laser (laser 2). This is simply $\pi r_2^2 l$, where r_2 is the beam radius of laser 2 and l is the diameter of the aperture through which the ions pass into the TOF drift tube. Thus the quantity, I_{Na^+} in Eq. (8) is the integrated ion signal divided by $\pi r_2^2 l$. If radiation trapping did not occur the collection volume for Na_2^+ would be given by a similar factor for laser 1. However, the effect of radiation trapping is to enlarge the excited volume of Na $3p$ atoms. This leads to a larger effective volume over which Na_2^+ is produced and collected. In order to determine the actual volume of excited atoms we use the uv beam as a photoionizing probe. First we introduce laser 2 at 90° to laser 1 and vary its position (horizontally and vertically) while monitoring the intensity of Na^+ produced from photoionization of excited atoms. Next we perform the same measurement with laser 2 introduced collinearly with laser 1 (see Fig. 2). In this way we obtain a three-dimensional spatial distribution of Na $3p$ population. The quantity $I_{\text{Na}_2^+}$ in Eq. (8) is then obtained by dividing the Na_2^+ ion signal by this volume.

In the last part of the experiment we exploit another effect of radiation trapping—increase in the apparent lifetime of the excited-atom population—to determine the absolute Na $3p$ density in a way which is also nearly independent of all apparatus constants. A recent report by Garver *et al.*,⁹ based on the earlier work of Milne,⁸ describes a general method for determining atomic number densities. The experimental work of Kibble *et al.*¹⁰ confirms the validity of Milne's theory in the density range 10^9 – 10^{13} atoms/cm³, which includes the experimental conditions reported here. Following Milne's method in the low-density limit, we express the ground-state density as

$$N = \left[\frac{\tau^*}{\tau} - 1 \right] (\omega \alpha)^{-1}, \quad (9)$$

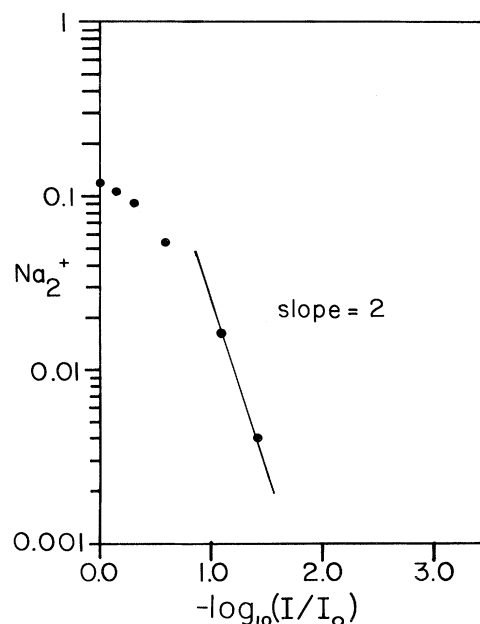


FIG. 4. Log-linear plot of the Na_2^+ signal (arb. units) vs fractional power of laser 1.

where τ is the natural lifetime of the excited level, α is the atomic absorption coefficient, and ω is the linear extent of the excited vapor. Our experimental conditions define $\omega = 0.64$ cm which is the separation between the TOF acceleration plate and the aperture to the drift tube. For sodium, $\tau = 16$ nsec and $\alpha(^2P_{3/2}) = 10^{-11}$ cm².¹¹ Thus Na $3s$ density is given by

$$[\text{Na}(3s)] = \left[\frac{\tau^*}{16} - 1 \right] (1.6 \times 10^{11}). \quad (10)$$

Under saturation conditions, the Na $3p$ density is equal to the Na $3s$ density (before irradiation) multiplied by a statistical factor. Because the number of M_j levels populated depends on the polarization of the exciting radiation, the factor is 0.5 if the radiation is linearly polarized and is 0.67 if it is unpolarized. In the present experiment the laser light is linearly polarized.

From laser-power measurements determined with a calibrated calorimeter, and the beam cross section of laser 2 defined by a 1-mm diaphragm, we obtain Φ in Eq. (8). The spot size of laser 2 was checked with a sensitive fluorescent screen placed directly at the interaction region. The photoionization cross section σ_i is taken from Aymar *et al.*¹² The time during which Na_2^+ is produced, Δt , is simply equal to the duration of the laser exciting the $^2P_{3/2}$ level plus the apparent lifetime τ^* , which we determine in the following way. Laser 1 is tuned onto the Na $3^2S_{1/2} \rightarrow 3^2P_{3/2}$ transition. Then laser 2 (uv), introduced collinearly at 180° to laser 1, photoionizes Na atoms in the $3p$ level. The apparent lifetime τ^* is measured by monitoring the decrease of the Na^+ signal versus the *time delay* between laser 1 and laser 2. We use a fast photodiode to display the temporal position of both lasers. With the falling edge of laser 1 at $t = 0$, we systematically

vary the delay of laser 2. A log-linear plot of the Na^+ signal versus Δt generates a straight line with a slope proportional to $1/\tau^*$ (Fig. 3). We use a series of calibrated neutral density filters to assure the proper dependence of the ion signals versus fractional laser power.

Figure 4 is a plot of the Na_2^+ signal versus fractional power of laser 1 and illustrates saturation of the signal at high power and a quadratic dependence at low power. Saturation of the $3p$ level is confirmed in a plot of the Na^+ signal generated by direct photoionization versus fractional power of laser 1 (Fig. 5). In addition, a plot of the Na^+ signal versus fractional power of laser 2 verifies the expected linear dependence with respect to the photoionizing laser (Fig. 6).

IV. RESULTS AND DISCUSSION

The rate constant for AI is calculated using Eq. (8). We find the average value to be (in units of cm³ sec⁻¹)

$$k = (1.8 \pm 0.7) \times 10^{-11}.$$

We calculate the uncertainty in the computed rate constant δk using a propagation of random-error analysis given by

$$\frac{\delta k}{k} = \left[\left(\frac{\delta I_{\text{Na}_2^+}}{I_{\text{Na}_2^+}} \right)^2 + \left(\frac{\delta I_{\text{Na}^+}}{I_{\text{Na}^+}} \right)^2 + \left(\frac{\delta \Phi}{\Phi} \right)^2 + \left(\frac{\delta[\text{Na}(3p)]}{[\text{Na}(3p)]} \right)^2 \right]^{1/2}, \quad (11)$$

where $\delta I_{\text{Na}_2^+}$, δI_{Na^+} , $\delta \Phi$, and $\delta[\text{Na}(3p)]$ represent the uncertainties in the measured ion signals, laser-power mea-

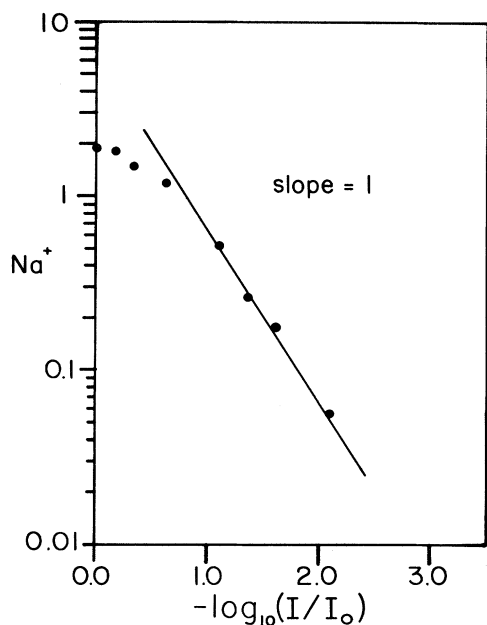


FIG. 5. Log-linear plot of the Na^+ signal (arb. units) vs fractional power of laser 1.

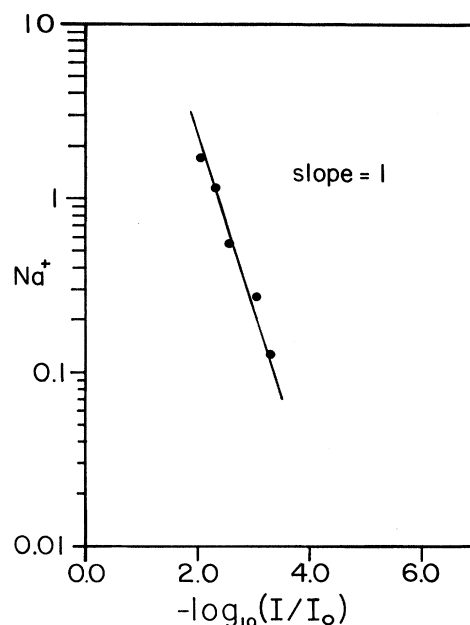


FIG. 6. Log-linear plot of the Na^+ signal (arb. units) vs fractional power of laser 2.

TABLE I. Comparison of measured cross sections for AI in collisions between Na 3p atoms.

Reference	Cross section (\AA^2)
1	$\sim 0.13^a$
3	0.05
4	10
14	0.73 ± 0.27^b 0.76 ± 0.28^c
This work	1.5 ± 0.6

^aAuthors report a rate constant of 1.3×10^{-12} cm³/sec. We have assumed a thermal velocity of $\sim 1 \times 10^5$ cm/sec to obtain the cross section.

^bCorrected Na²P_{3/2}-²P_{1/2} collisional mixing assuming $k_{3/2,3/2} = 4k_{1/2,1/2} = 2k_{3/2,1/2}$.

^cCorrected for Na²P_{3/2}-²P_{1/2} collisional mixing assuming $k_{3/2,3/2} = 2k_{3/2,1/2}$; $k_{1/2,1/2} = 0$.

surements, and Na 3p density determinations, respectively. Uncertainties in Δt and σ_i are negligible compared to these other contributions. The values of $\delta I_{\text{Na}_2^+}$ and δI_{Na^+} are calculated by the computer after a preset number of laser shots (usually 1000) along with the values of $I_{\text{Na}_2^+}$ and I_{Na^+} , and are on the order of 15%. The uncertainty in Φ is due to shot-to-shot fluctuations in the laser, which we estimate to be $\sim 25\%$. The major contribution to the uncertainty in [Na(3p)] arises from the determination of the effective volume of Na* 3p population where we estimate run-to-run variability of about 20%.

In addition to Na₂⁺ we observe a smaller Na⁺ signal which may be due to photodissociation of the ion dimer. Carré *et al.*¹³ have recently measured the cross section for Na₂⁺ photodissociation. Using their result along with the measured power density of laser 1, we calculate the expected loss of Na₂⁺ to be no greater than 10%. This is consistent with the magnitude of observed Na⁺ intensity.

For a beam temperature of ~ 575 K, the average relative velocity of the colliding atoms is 1.2×10^5 cm/sec. Using $\sigma = k / \langle v_{\text{rel}} \rangle$, we obtain a cross section of $\sim 1.5 \text{ \AA}^2$. Table I compares the present result with other studies. Of particular interest is the recent work of Huennekens and Gallagher¹⁴ who measured the AI rate constant at higher pressure (5.6×10^{14} cm⁻³) where Na²P_{3/2} and Na²P_{1/2} are statistically mixed by collisions with ground-state atoms. The average rate constant $\langle k \rangle$ can be written in

terms of the separate rate constants associated with the two fine-structure levels and their fractional populations as

$$\langle k \rangle = k_{3/2,3/2} f_{3/2}^2 + k_{1/2,1/2} f_{1/2}^2 + 2k_{3/2,1/2} f_{3/2} f_{1/2}, \quad (12)$$

where $k_{3/2,3/2}$, $k_{1/2,1/2}$, and $k_{3/2,1/2}$ are the AI rate constants for collisions between atoms in the Na²P_{3/2}, Na²P_{1/2}, and Na²P_{3/2}-Na²P_{1/2} levels, respectively. The terms $f_{3/2}$ and $f_{1/2}$ denote the fraction of Na 3p population in the ²P_{3/2} and ²P_{1/2} levels, respectively. Assuming statistical population mixing, we rearrange equation (12) to express $k_{3/2,3/2}$ as

$$k_{3/2,3/2} = 2.25 \langle k \rangle - 0.25 k_{1/2,1/2} - k_{3/2,1/2}. \quad (13)$$

In the crossed-beam results reported here, statistical mixing is zero, and the AI rate constant is $k_{3/2,3/2}$. To compare $\langle k \rangle$ measured by Huennekens and Gallagher with $k_{3/2,3/2}$ reported here, we use (13) and assume values for $k_{1/2,1/2}$ and $k_{3/2,1/2}$. Although we did not make careful measurements of $k_{1/2,1/2}$ we noted in the course of experiments that $k_{1/2,1/2} \sim \frac{1}{4} k_{3/2,3/2}$. If we posit this value and assume (rather arbitrarily) that $k_{3/2,1/2} = (k_{1/2,1/2} k_{3/2,3/2})^{1/2}$ we calculate $k_{3/2,3/2} = (0.81 \pm 0.30) \times 10^{-11}$ cm³sec⁻¹ which is to be compared with $(1.8 \pm 0.7) \times 10^{-11}$ cm³sec⁻¹ reported here. Table I shows the corresponding cross sections. Although the comparison requires two *ad hoc* assumptions, the entries in Table I show that $k_{3/2,3/2}$ calculated from Ref. 14 is not too sensitive to them. We note that despite entirely different techniques used to measure the AI rate constant, the error bars in the two determinations overlap; and considering that earlier determinations varied over 2 orders of magnitude, we judge the agreement satisfactory. A more solid comparison will have to await direct measure of $k_{1/2,1/2}$ and $k_{1/2,3/2}$ in future single-collision experiments.

ACKNOWLEDGMENT

This work was supported in part by National Science Foundation Grant No. PHY-83-05086.

*Permanent address: Institut d'Electronique Fondamentale, Bâtiment 220, Université de Paris—Sud F-91405 Orsay, France.

¹V. S. Kushawaha and J. J. Leventhal, Phys. Rev. A **25**, 346 (1982).

²V. S. Kushawaha and J. J. Leventhal, Phys. Rev. A **22**, 2468 (1980).

³A. deJong and F. van der Valk, J. Phys. B **12**, L561 (1979).

⁴A. Klucharev, V. Sepman, and V. Vuinovich, Opt. Spektrosk. **42**, 588 (1977) [Opt. Spectrosc. **42**, 336 (1977)].

⁵T. B. Lucatorto and T. J. McIlrath, Appl. Opt. **19**, 3948 (1980).

⁶M. Allegrini, G. Alzetta, A. Kopystynska, L. Moi, and G. Orriols, Opt. Commun. **19**, 96 (1976).

⁷J. Boulmer and J. Weiner, Phys. Rev. A **27**, 2817 (1983).

⁸E. Milne, J. London Math. Soc. **1**, 1 (1926).

⁹W. P. Garver, M. R. Pierce, and J. J. Leventhal, J. Chem. Phys. **77**, 1201 (1982).

¹⁰B. P. Kibble, G. Copley, and L. Krause, Phys. Rev. **153**, 9 (1967).

¹¹A. C. G. Mitchell and M. W. Zemansky, *Resonance Radiation and Excited Atoms* (Cambridge University Press, New York, 1934).

¹²M. Aymar, E. Luc-Koenig, and F. Combet Farnoux, J. Phys. B **9**, 1272 (1976).

¹³B. Carré, *Photon-Assisted Collisions and Related Topics*, 2nd ed. (Harwood Academic, London, in press).

¹⁴J. Huennekens and A. Gallagher, Phys. Rev. A (in press).